JOURNAL OF CRITICAL REVIEWS

ISSN- 2394-5125 VOL 7, ISSUE 01, 2020

Neural network controller based a Quasi-Z-Source Cascaded Four-Level Inverter for Photovoltaic Applications

[1]Mrs. P.Saraswathi Assistant Professor, saru.palem@gmail.com

[2]Mr. Venkateswar Rao Assistant Professor, venkatsnmpkmm@gmail.com

[3]Mr. V.Saidulu Assistant Professor pecsaidulu.eee@gmail.com

Department-EEE

Pallavi Engineering College Hyderabad, Telangana 501505

Abstract: This project's main objective is a Quasi-Z-Source Cascaded Four-Level Inverter for Photovoltaic Applications using a Neural Network (NN) controller. Three Quasi-Z-source (QZS) networks make up the power converter, which also includes a four-level cascaded multilevel inverter. The proposed topology is structurally simpler and has fewer components than traditional multilevel inverter configurations like cascaded H-Bridge inverters and neutral-point clamped inverters. While reducing the voltage stress on the switching devices, the proposed power converter and its modulation scheme increase the boost factor by 50% when compared to topologies. By altering the QZS networks' shoot-through duty ratio, it is demonstrated that the proposed converter can regulate the output voltage in the stand-alone mode. Additionally, it is demonstrated that the suggested converter with neural network control strategy can interface with the grid to accomplish PSO-MPPT (Particle Swarm Optimization Maximum Power Point Tracking) and UPF operation with the grid goals. The suggested simulation results validate the steady-state and dynamic performances of the suggested power circuit configuration and the corresponding control strategy.

Keywords: Photovoltaic (PV), PSO-MPPT, Neural Network (NN), Cascaded H-Bridge inverter, Quasi-Z-Source (QZS)

I.INTRODUCTION

The meaning of nonconventional energy sources is creating as conventional supplies quickly exhaust all through the globe. The regular improvement moved the progression of sun arranged photovoltaic (PV) structures. Sun arranged energy is being used to run all that from water siphons and streetlights to environment control frameworks and coolers. Sun arranged energy systems have become all the more notable as their worth, lifetime, and upkeep essentials have decreased lately. Any Course Age (DG) structure ought to have photovoltaics as a middle part. Medium-sized and more unassuming close by planet gatherings may either work alone or interact with the cross section. Due to the by and large low voltages seen at the sheets' outcome, inverters are as often as possible used in daylight-based PV systems to create AC at the important voltage and repeat. For the most part, this is a two-stage change process. To begin, a DC help converter takes the to some degree low DC voltage yield from the PV sheets and lifts it to the vital DC voltage level. The usable voltage is extended and most outrageous power point following is made possible by this converter, making it an essential piece of any sun based photovoltaic system. Then, a standard voltage source inverter changes the escalated DC voltage into AC power at the predefined voltage and repeat (VSI). In any case, the two-stage change approach generally extends the cost and multifaceted design of the power circuit [1-2], it is still extensively used. By relationship, a standard VSI in a lone stage DC/AC converter prompts an overengineered structure plan [3]. (Which, even with lower PV voltage, should give the essential AC voltage). The Z-source inverter (ZSI) is a single stage power circuit plan that might be used to evade these cut-off points. Low PV voltage over a wide voltage range is maintained, and it has fundamental protection from the shoot-through deficiency [4-5]. qasr inverters address the issue of a discontinuous data current, which plagues ordinary ZSIs [6]. Diverged from standard ZSIs, skis partake in an additional advantage in that one of the capacitors has an impressively lower voltage rating. Anyway, PV systems every now and again consolidate MLIs (multi-layer inverters). Their outcome voltage waveforms are clearer on semiconductors than those of standard two-level VSIs with respect to Amount to Consonant Bending (THD), EMI, and dv/dt. Along these lines, a qasr network with multi-layer inverters could obtain the benefits of the two geologies [7, 8]. Different researches on Source

ISSN- 2394-5125 VOL 7, ISSUE 01, 2020

and multi-layer inverter blend have focused in on the more normal NPC and CHB converter topographies. According to the assessments presented in [9, 10], the normal buck-help cut-off may be accomplished by partner two DC sources to two Z-sources. The excessively long DC-interface closes at an NPC Staggered Point of connection (MLI) that offers three levels of affiliation. The Source is constrained by a standard single-stage game plan, with the shoot-through period of time given by a three-level inverter at the system's posterior. Source associations may be more over the top to adapt to shoot-through since additional cut-out diodes and a muddled equilibrium system are required. To execute the single Z-source course of action from [11], two DC sources are required. Instead of [9], it basically needs a single association of impedances. Extensions in size and part assessments in the uninvolved parts are made while keeping the structure's esteeming something basically the same. These enhancements have incited the creation of a lot of elective power circuit designs that rely upon a singular DC supply and a lone Z-source [12]. The key issue of these geologies is that they need a consistent data current, which isn't alluring for PV systems. Three-stage qasr-NPC geologies were composed [13] to safeguard a consistent data current. The resultant geology of a fair blend of two qasr networks is a T-type structure with a run of the mill objective point. In [14], it is shown that an uncommon arrangement considering changed qasrs could enhance the power circuit overall. Two qasr networks join a trio of T-level inverters to make this power converter. Issues emerge while standing apart these geologies from the conventional qi, recollecting that I am clumsiness for the capacitor voltages that changes the fair-minded point voltage, (ii) the need for extra fastening diodes, and (iii) no improvement in help factor. [13] [14]. With a Streamed H-Platform Staggered Inverter (CHB-MLI), each individual H-range inverter unit helps with reducing the DC-interface voltage anticipated by the whole inverter system. Both unquestionably the consonant mutilation (THD) and the dv/dt (time assortment) of the outcome voltage waveform have been essentially better [15-17]. It has been proposed lately ([18,19]) that combining CHB-MLIs with qasrs is a useful strategy. The fundamental voltage support is given by various H-length inverters, all of which is related with its own qasr association. To ensure genuine action of the DC-interface and MPPT, the voltages for each ought to be kept completely isolated from one another [20, 21]. Nine individual PV sources, 36 semiconductor trading contraptions, and entryway drive circuits are supposed to comprehend the single-stage, three-stage qasr-CHB MLI proposed in [20]. Growing the amount of outcome voltage levels makes the qasr-CHB MLI converter more successful, but it similarly makes staying aware of control truly testing and expensive. Since controlling the dc-associate voltage of each qasr and doing most outrageous power point following is major anyway dreary. The Streamed Staggered Inverter is an extraordinary device that thinks about simultaneous inversion at a couple of levels (CMI). When diverged from the CHB-MLI structure, this one calls for evidently less DC sources and trading contraptions. The CMI MLI configuration doesn't need fastening diodes or capacitors, rather than the NPC and FC geologies. While the outcome voltage waveform stays unaltered, the size of the DC power supply and the amount of power semiconductor trading devices can be decreased by using CMIs. Due to the diminished number of moving parts, a CMI might perhaps be more dependable than the recently referenced power converter structures. This study proposes another power converter plan that uses qasr networks connected with a Four-level CMI to perform single-stage change. This concentrate in like manner shows that the proposed converter's aiding limit is duplicated when offset with a carrier-based Level shifted Space Vector Heartbeat Width Guideline (LSPWM) plot, conversely, with the supporting furthest reaches of NPC 3-level and CHB-based structures. The proposed converter beats the recently referenced geologies across the repeat range since it has more possible levels of result voltage. It is in like manner shown that the FCMI is utilized by the proposed LSPWM plan to supply the shoot-through condition expected by the qasr without adding to any additional influence setback in the semiconductor trading devices. The proposed converter's reliable state and dynamic execution are penniless down through proliferation studies.

II . PROPOSED POWER CONVERTER

ISSN- 2394-5125 VOL 7, ISSUE 01, 2020

Figure 1 is a schematic of the proposed qasr-based four-level flowed staggered inverter, which would be fuelled by photovoltaic cells. Three 2-level voltage source inverters are flowed in this circuit to deliver a 4-level reversal. To work in shoot-through mode, qasr networks need two of these inverters. Subsequently, the STI-1 and STI-2 renditions are known as Shoot-Through Inverters. To coordinate the result of the two shoots through inverters toward the heap/framework, the DC input terminals of the third VSI are associated with the terminals A1, B1, and C1 of STI-1 and STI-2, separately. This idea shapes the premise of the result inverter.

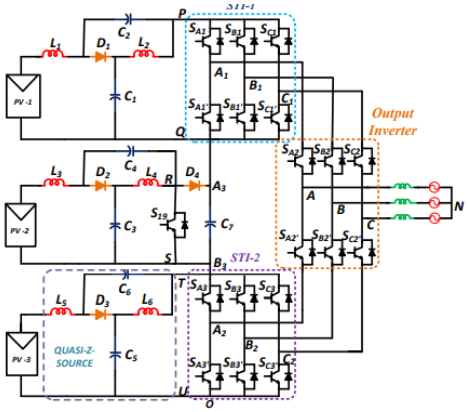

Fig.1. Proposed qasr-FCMI

These VSIs are controlled by three closely resembling qasr organizations, which help the deficient voltage from the conveyed PV boards to a suitable level. The core of a qasr network comprises of a switch (S19), a capacitor (C7), and a diode (D7) (D4). These parts need a steady DC voltage supply at their terminals (A3, B3). The qi might be utilized in two unmistakable ways, similar as a traditional Z-source inverter: I in a shoot-through design, and (ii) in a non-shoot-through setup. Sunlight based chargers and capacitors (C1, C2) store energy until the stage switches are turned on, permitting the inverter to work (L1, L2). At the point when qi isn't working in shoot-through mode, it sends the power put away in the inductors to the heap. Options in contrast to dead-band hardware for forestalling shoot-through incorporate putting impedance networks before the inverters. The power semiconductor exchanging gadgets (S1-S19) in this plan are exceptional (S1-S19). The shoot-through mode is acknowledged by means of the phase legs of the STI-1 and STI-2 inverters for both the upper and lower semi-Z-sources. An extra switch (S19) in the focal qasr enacts shoot-through mode.

SWITCHING STATES AND THE OUTPUT VOLTAGE OF THE FOUR-LEVEL INVERTER

The VAO, VBO, and VCO images in Fig. 1 address the shaft voltages of the qasr four-level inverter, and their particular states are talked about in Segment 5.2 of this paper. In Table I, you can see the post voltage and exchanging states for every gadget that comprises the A-period of the proposed FCMI. The proposed power converter's exchanging gadgets are addressed as 1s and 0s, separately, in Table I and the remainder of the paper. The proposed converter can work as a four-level VSI because of the way that the voltage at each post can take on one of sixteen distinct qualities (Table I).

TABLE I POLE VOLTAGE (V_{AO}) FOR DIFFERENT SWITCHING COMBINATION

State type	Pole Voltage (V_{AO})	Level No	Pole (A) terminal connection (See Fig.1)	Switching states (1-ON, 0-OFF)					
				S_{A1}	$S_{A1'}$	S_{A2}	$S_{A2'}$	S_{A3}	$S_{A3'}$
NST	V_{DC}	3	P	1	0	1	0	0	0
NST	$\frac{2V_{DC}}{3}$	2	Q	0	1	1	0	0	0
UST				1	1	1	0	1	0
NST	$\frac{V_{DC}}{3}$	1	T	0	0	0	1	1	0
NST	0	0	U	0	0	0	1	0	1
LST				0	1	0	1	1	1

*NST-Non shoot-through,*UST-Upper shoot-through,*LST-Lower shoot-through.

Table I likewise shows the different exchanging conditions of the STI-1 and STI-2 inverters during stage A shoot-through. At the point when a shoot-through state is brought into a STI-1 stage, the shaft voltage drops from VDC to 2VDC/3, as displayed in the table. At the point when a shoot-through state is enacted, the post voltage for a phase leg in the STI-2 portrayal drops to 0 V. The post voltages of a four-stage flowed qasr inverter are displayed as:

$$V_{AO} = S_{A2} * S_{A1} + \frac{(S_{A2'} * S_{A3})}{3} + \frac{(S_{A1'} * S_{A2}) * 2}{3} \quad (1)$$

$$V_{BO} = S_{B2} * S_{B1} + \frac{(S_{B2'} * S_{B3})}{3} + \frac{(S_{B1'} * S_{B2}) * 2}{3} \quad (2)$$

$$V_{CO} = S_{C2} * S_{C1} + \frac{(S_{C2'} * S_{C3})}{3} + \frac{(S_{C1'} * S_{C2}) * 2}{3} \quad (3)$$

ISSN- 2394-5125 VOL 7, ISSUE 01, 2020

Common mode voltage will be the average of three-pole voltages as shown

$$V_{CM} = (V_{AO} + V_{BO} + V_{CO})/3 \quad (4)$$

Phase voltage of the inverter using the above equations

$$V_{AN} = V_{AO} - V_{CM} \quad (5)$$

$$V_{BN} = V_{BO} - V_{CM} \quad (6)$$

$$V_{CN} = V_{CO} - V_{CM} \quad (7)$$

Thus, the phase voltages are expressed as:

$$V_{CN} = (2*V_{CO})/3 - (V_{BO}/3) - (V_{CO}/3) \quad (8)$$

$$V_{AN} = (2*V_{AO})/3 - (V_{BO}/3) - (V_{CO}/3) \quad (9)$$

$$V_{BN} = (2*V_{BO})/3 - (V_{CO}/3) - (V_{AO}/3) \quad (10)$$

OPERATION OF THE CONVERTER

Ordinarily, post an is connected to the letter Q, shaft B to the letter T, and shaft C precisely - U, as found in Figure 2. (a). More specifically, when the vector [210] is flipped, every one of the three STI-1 result focuses (A1, B1, C1) are braced to the negative rail of the top qasr organization (for example the STI-1 is worked with an invalid vector). The STI-1 shoot-through circumstance is prompted accordingly, as displayed in Fig.2. (a). In the event that we take a gander at Fig.2(b), we can see that the mood killer of the base gadget SA1' is unaffected (i.e., it actually happens at 't1' as in the past), while the rising edge of the gating sign to the top-gadget SA1 is advanced by a length of 3Tsh/2. In this way, the changing power misfortune didn't build because of the consideration of the shoot-through condition. Shaft An is associated with terminal P on STI-1, Post B is associated with terminal T on STI-2, and Shaft C is associated with terminal U on STI-2 in the state [310], as displayed in Fig.5(b). For this reason, STI-1 and STI-2 are both on and the result inverter is providing the heap with power from the oz. sources. In Fig.2, the shafts A, B, and C are shown associated with the "P," "Q," and "U" terminals, separately, in the [320] condition of the proposed converter. This is reliable with the perception that STI-1 and STI-2 are both useful in the state [310]. The DC-connect in the top qasr organization will be reinforced if a shoot-through happens during STI1's A stage. The shoot-through time (ST) is separated equitably between STI-1 and STI-2 to ensure typical activity of the top-and base qasr networks over a consistent example time span (Ts). By flipping the vector, the STI-2 can be placed into a zero-vector mode [321]. Figure.2 shows the positive rail of the base qasr network braced to the three STI-2 result terminals (A2, B2, and C2). The shoot-through condition might be started with a straightforward flip of switch SC3' when used in mix with this setup. From what has been talked about, obviously the middle segment of the qasr can't be utilized to present the shoot-through condition as of now. To make up for the generally low voltage yield from the centre string, a subsequent switch (S19, Fig. 1) is given to initiate the shoot-through state.

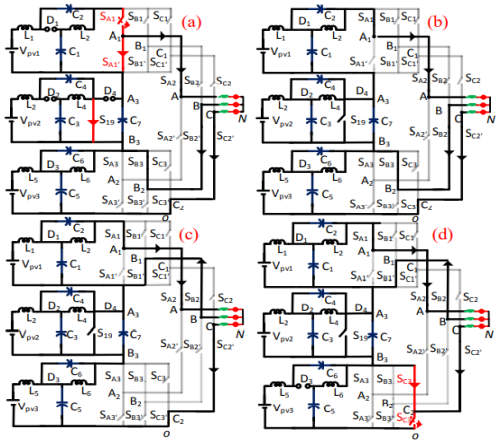

Fig. 2 Circuit diagrams for switching states (a) [210] state (b) [310] state (c) [320] state (d) [321] state in a given sample time Ts.

III. CONTROL SCHEME OF QZS-FCMI FOR STANDALONE AND GRID CONNECTED OPERATION

Stand-alone mode

ISSN- 2394-5125 VOL 7, ISSUE 01, 2020

To decide the proposed converter's general increase, we duplicate the lift factor (B) of the front-end qasr segment by the regulation file (M) of the back-end 4-level inverter. It's not difficult to perceive how these two parts supplement each other. The DC-connect for the 4-level inverter comes from the front-end qasr, and the shoot-through state is given by the back-end qasr. To forestall the concise short-circuiting of the DC-connect brought about by the shoot-through state from mutilating the waveform of the result voltage from the 4-level inverter, the shoot-through state is presented during the invalid change. Tweak record (M), which decides the result voltage of a 4-level inverter in independent mode, is ordinarily fixed. The lift factor (B) of the qasr is changed in light of DC-connect voltage changes acquired on by varieties the PV voltage, considering shut circle guideline of the 4-level inverter's result voltage. Since the lift factor (B) and the shoot-through obligation factor are contrarily corresponding to each other, it is adequate to control the shoot-through obligation apportion ('D') alone to lay out the proper result voltage. The control strategy for managing the DC-connect voltage of a 4-level inverter utilizing the shoot-through obligation proportion is displayed in Fig. 3. A beating voltage waveform is created at the DC-interface terminals when the shoot-through mode is brought into each stage leg of the STI-1 and STI-2 inverters. This is on the grounds that the DC-joins are provided by qasr organizations (terminals P, Q, R, S, and T, U as set apart in Fig. 5.1).

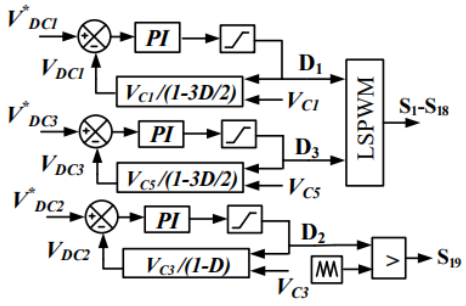

Fig. 3 DC-link voltage control scheme for the proposed FCMI.

This beating waveform isn't promptly recognizable thus can't be used as the criticism sign to control the DC-connect voltage, as displayed in Fig. 1. We might gauge the voltage across the DC association by checking the voltage across the capacitors and the shoot-through obligation proportion (D). At the point when the DC-connect voltages VDC1 and VDC3 don't match their reference values, blunders are shipped off the PI regulators. Shoot-through obligation proportions "D1" and "D3" are changed utilizing control signals from PI regulators. The LSPWM framework might utilize the obligation proportion signs to create the gating signals for STI-1 and STI-2. Obligation proportion ('D2') is utilized to control the DC-interface voltage of the Result Inverter, and a switch ('S19') embeds a shoot-through condition for the middle of the road qasr (Fig. 5.3). Reliable, controlled yield voltage for the end client is ensured through shut circle criticism guideline of the inverters' three pinnacle DC-connect voltages (VDC1, VDC2, and VDC3).

Grid connected mode

The FCMI should make the accompanying strides to lay out an association with the matrix: To start, every one of the three qasr networks needs their own MPPT control, the UPF should be kept in a state of harmony with the lattice, and the DC-connect voltage should be observed and controlled. Boundaries D (the shoot through obligation proportion) and M (the regulation file) oversee the proposed converter's way of behaving, with D alone liable for acknowledging Objective 1 and M exclusively responsible for acknowledging Objectives 2 and 3, separately (M). The converter matrix mix block format is displayed in Fig. 8. To get the most energy out of the PV cells, the well-known Molecule Multitude Improvement (PSO) strategy is utilized. Three photovoltaic (PV) sources' voltages and flows are followed and shipped off their different PSO-MPPT regulators with the goal that the shoot-through obligation proportion still up in the air (D1, D2, and D3). Shoot-through obligation proportions D1 and D3, which are indistinguishable from D under consistent state conditions, are contribution to the LSPWM framework to screen the greatest power from the top and base PV sources, individually (Fig. 4). Switch S19 directs the span of the shoot-through in the middle qasr organization. Maximal power point checking for PV-2 is subsequently empowered by changing the obligation proportion

ISSN- 2394-5125 VOL 7, ISSUE 01, 2020

of switch S19. Exclusively by approximating the voltages of every individual DC interface, which we'll allude to as VDC1, VDC2, and VDC3, can the FCMI's all-out DC-connect voltage (Vectoral) be controlled. Comparably to independent activity, the DC-interface still up in the air by detecting the voltages and obligation proportions across the capacitors (Vectoral). The DC-connect voltage is contrasted with its reference (V* doctoral) by the NN regulator in the external voltage circle, and the outcome (the d-hub reference current I'd) is shipped off the inward current circle. A power variable of 1 requires the q-pivot part I q) to be zero. The necessary adjustment list () is found by contrasting the reference flows (id, intelligence level) with the d-and q-parts of the lattice flows (acquired by means of Park's change to the 3-stage flows).

To create the regulating signals for the "ABC" stages, the Converse change Park's takes as sources of info the d-q reference voltages (V* d, V* q). The balancing signals and the matrix can be kept in a state of harmony with the assistance of a stage locked circle. With the assistance of these balancing signals, the LSPWM conspire is executed, which thusly produces the gating signals important for the power semiconductor exchanging gadgets in the FCMI.

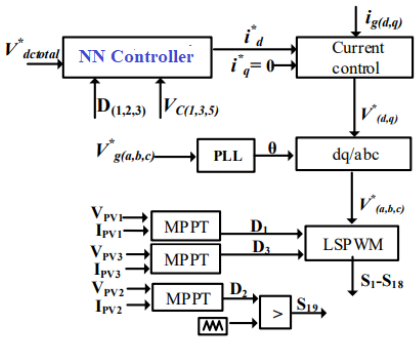

Fig. 4 Block diagram of grid control scheme

IV. PROPOSED ANN CONTROLLER

The offline trained Neural Network (NN) controller with supervised learning for the grid control is shown in fig (5).

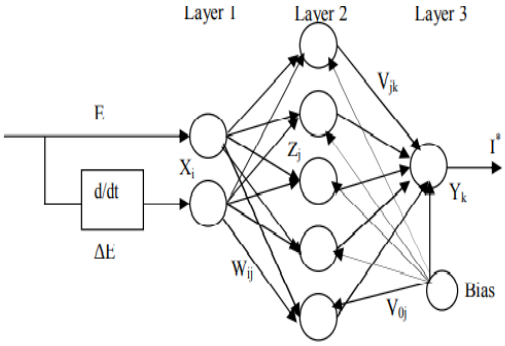

Figure 5 Neural network control system

To limit the following mistake between the reference current (I*) and the genuine current (I), the NN regulator's associating loads are prepared utilizing the blunder € and the pace of progress of mistake € €. The utilization of NNs in modern control frameworks considers more exact forecast and guideline, speedier reaction times, and improved commotion dismissal. The covered layer comprises of five neurons (Xi+1): two info neurons (Xi) and four result neurons (Ky). Neurons in a single layer converse with neurons in the following layer across associations with loads that change from one neuron to another thanks to the utilization of antimonide and purlin enactment capabilities for the covered up and yield layers, separately. A brain network model has been prepared utilizing data from customary regulators.

PSO MPPT

An intelligent optimization theory, particle swarm optimization (PSO) was developed by Eberhart and Kennedy in 1995. It employs a swarm of microscopic particles to find optimal solutions to problems. The idea behind this algorithm was to tackle the search and optimization problems that plagued earlier algorithms; it took its cue from the foraging behaviour of birds and schools of fish. Each particle's location and velocity inside the search region are updated at each iteration, creating the appearance that the particles are traveling together like schools of fish or flocks of birds. In addition to the Best awarded to the best particle, each participant also received a Pest as well as a distance and a direction to go. As can be seen in

ISSN- 2394-5125 VOL 7, ISSUE 01, 2020

fig. 7, once the maximum number of iterations is achieved or the particle velocity reaches zero, the algorithm stops.

$$V_i(K+1) = w.V_i(K) + c_1 r_1\left(P_{best} - x_i(K)\right) + c_2 r_2.\left(G_{best} - x_i(K)\right) \quad (5.11)$$

$$x_i(K+1) = x_i(K) + V_i(K+1) \quad (5.12)$$

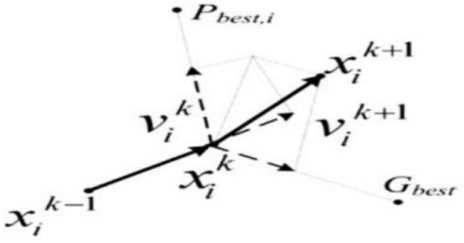

Figure .6 The movement of particles

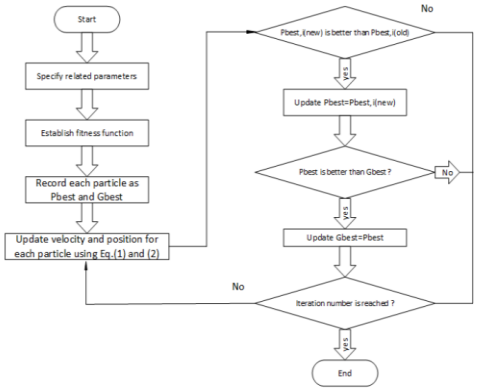

Figure 7: flowchart of conventional PSO

From the equations above, we can deduce that each iteration involves updating the particle's position and speed until the maximum power of the PV module is achieved.

Pbest: Personal best position for the particle itself

Gbest : Global best position among all particles

xi : The location of particle

vi:The velocity of the particle

*r*1,*r*2:Random numbers between [0,1]

K: number of iterations

*c*1,*c*2: Cognitive and social coefficient respectively

W: inertia weight

V.SIMULATION RESULTS

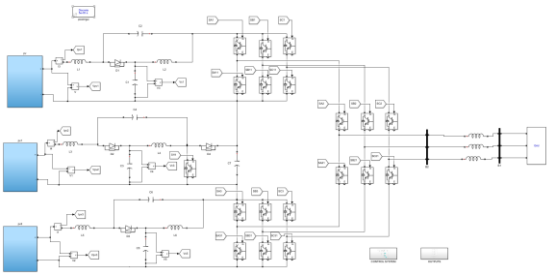

Fig.8 MATLAB/SIMULINK circuit diagarm of the system

A)EXISTING RESULTS

In Fig. 9, we see (a) the info voltage, (b) the DC-connect voltages for STI-1 and STI-2, and (d) the result inverter. DC-connect voltages at both the top and base hubs might show beats with amplitudes between 0 V and 243 V. The DC-connect voltage of the impacted inverter will drop to nothing if shoot-through happens in the stage legs of the STI-1 or STI-2. The DC-connections of these two inverters read 243V while working in power move mode. C7, a capacitor in the middle qasr organization, gives a consistent 243 V to the DC contribution of the result inverter. As referenced over, these discoveries confirm the hypothetical investigation's forecast that the DC-connect voltages will be 250 V.

ISSN- 2394-5125 VOL 7, ISSUE 01, 2020

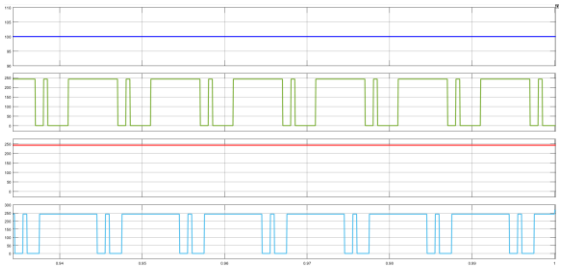

Fig. 9 Simulation results of (a) input voltage of single PV source (Vin1) (b) boosted DC-link voltage of STI-1(Vdc1) (c) boosted DC-link voltage of output inverter (Vdc2) (d) boosted DC-link voltage of STI-2 inverter (Vdc3).

Figure.10 displays the inductor currents of the top, middle, and bottom quasi-Z-sources in the same sequence. Capacitor C1 and C3 have simulated voltages of 172 V and 72 V, respectively, that are very close to their theoretical values.

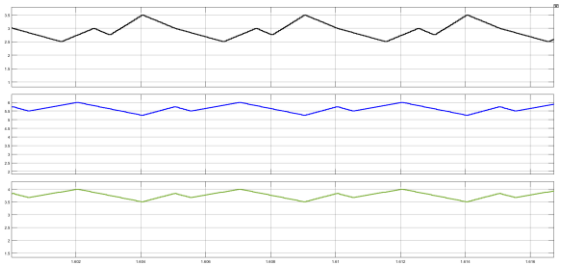

Fig.10 Simulation results of (a) inductor current (iL1) (b) Inductor current (iL3) (c) Inductor current (iL5).

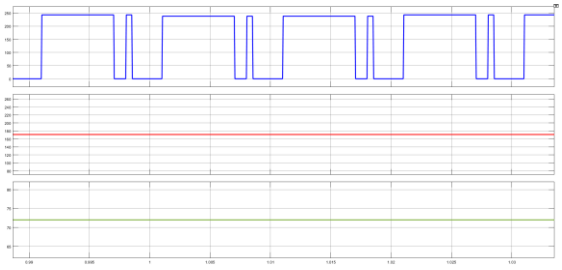

Figure.11 shows the calculated voltages (Vc1 and Vc2) between the capacitors and the DC connection (Vdc1).

The DC interface voltage control's relentlessness is tried by keeping the voltage across each of the three PV inputs at a consistent 100 V. As the heap obstruction is unexpectedly expanded, the heap current diminishes by almost half. Figure 12(a) portrays the information voltage of the FCMI, while Figures 12(b), 12(c), and 12(d) portray the voltages of the three DC joins. Figures 12(e) and 12(f) show the stage voltage and current separately.

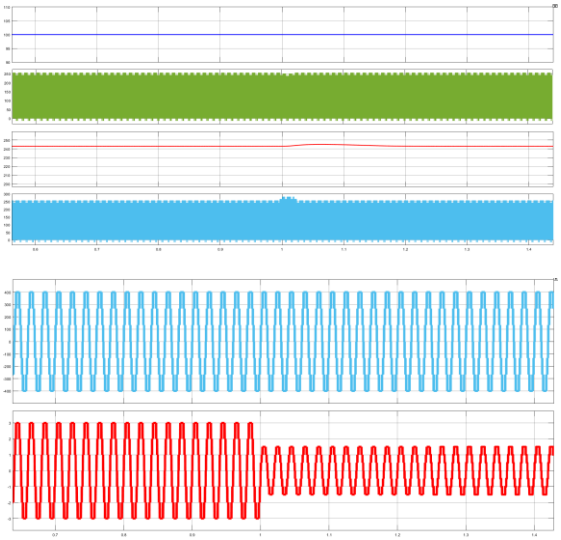

Fig. 12 Simulation results of (a) input voltage (Vin1) and DC-link voltages (b) Vdc1, (c) Vdc2, (d)Vdc3 of FCMI during load variation (e) phase voltage and (f) phase current of FCMI during load variation.

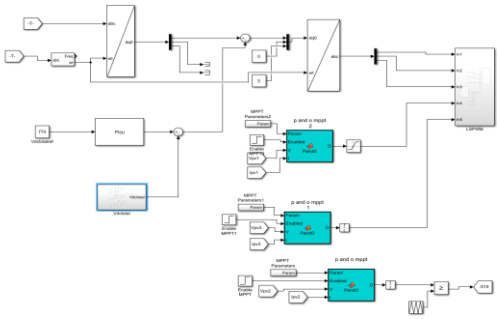

Fig .13 Grid control system

A graphical portrayal of the source variety and the mimicked voltages at the information sources (Vin1, Vin2, Vin3) and DC-connect is displayed in Fig 13. By changing the shoot through obligation proportions ('D1', 'D2', and 'D3'), the MPPT control method permits the sunlight-based charger to work at its most extreme power point (MPP) when exposed to an unexpected increment or lessening in

ISSN- 2394-5125 VOL 7, ISSUE 01, 2020

irradiance (from 700W/m2 to 1000W/m2 in 2.5 sec).

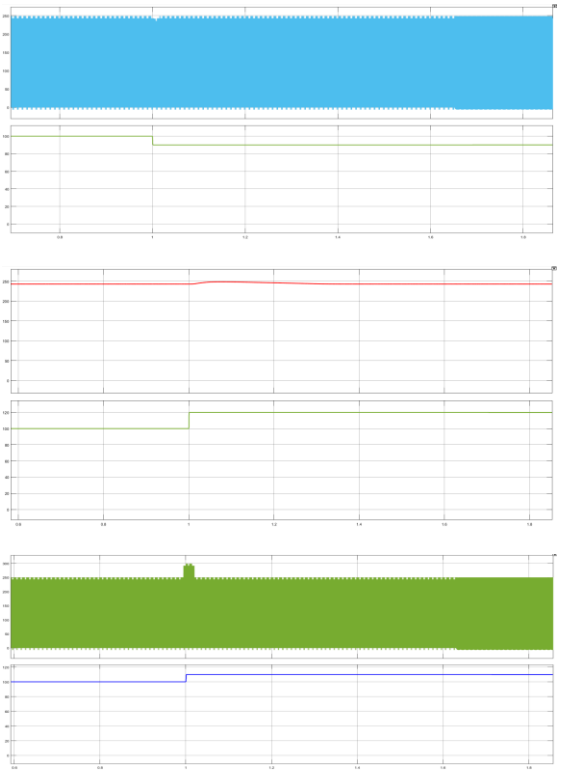

Fig.14 Simulation results of Input voltages (Vin1, Vin2, Vin3) and DC-link voltages (Vdc1, Vdc2, Vdc3) for source variation.

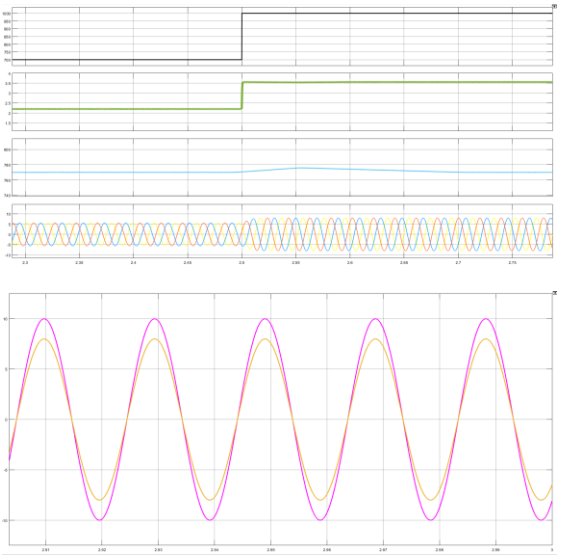

Fig. 15 Simulation results of (a) step change in irradiance (b) PV current (IPV1) (c) Total DC-link voltage (Vectoral) (d)Grid currents (Gab). (e) Grid voltage (Vega) and grid current (Igga).

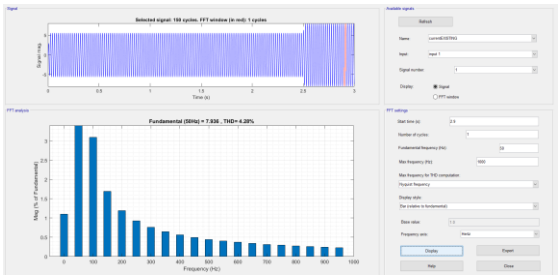

Fig.16 THD% Grid current

B) EXTENSION RESULTS

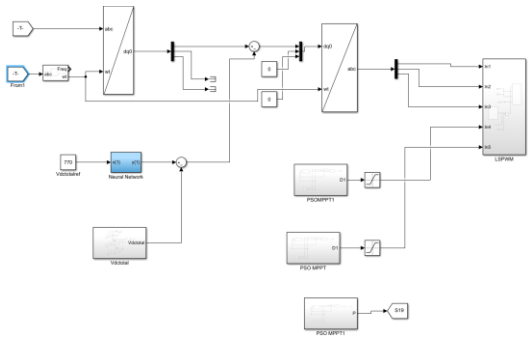

Fig .17 Grid control system with PSO MPPT and Neural Network controller

Figures 18 and 19 show how the proposed MPPT control technique changes the shoot through obligation proportions ('D1', 'D2', and 'D3') until the greatest power point (MPP) is achieved when a stage change in illumination is applied (from 700W/m2 to 1000W/m2 in 2.5 sec) and (from 500W/m2 to 700W/m2 at 2sec and 1000W/m2 in 2.5 sec). The DC-connect voltage control is graphically shown. 18(c) and 19(c) . Power assortment at UPF ascends with expanding insolation, as found in Figures 18(d) and 19(d), 18(e) and 19(e). The general symphonies twisting of the framework current in the proposed framework is displayed in Fig.20. In the similar table, obviously the proposed technique enormously brings down the THD% of framework current.

ISSN- 2394-5125 VOL 7, ISSUE 01, 2020

CASE-1 (irradiance 700 to 1000W/m^2)

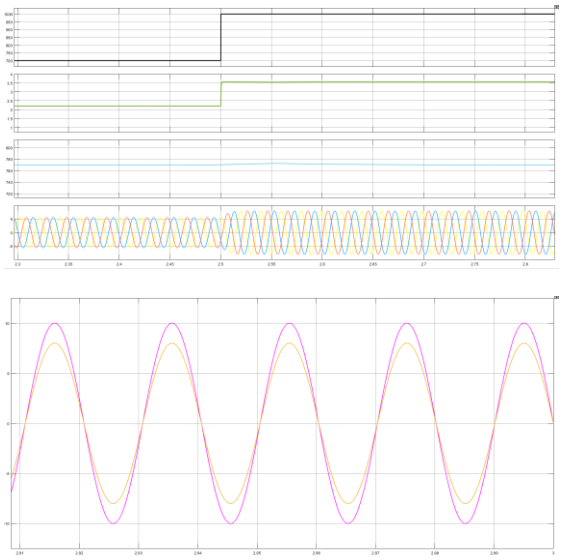

Fig.18 Simulation results of (a) step change in irradiance (b) PV current (IPV1) (c) Total DC-link voltage (Vectoral) (d)Grid currents (Gab). (e) Grid voltage (Vega) and grid current (Igga) at 1000 W/m^2

CASE-2 (irradiance 500, 700 to 1000W/m^2)

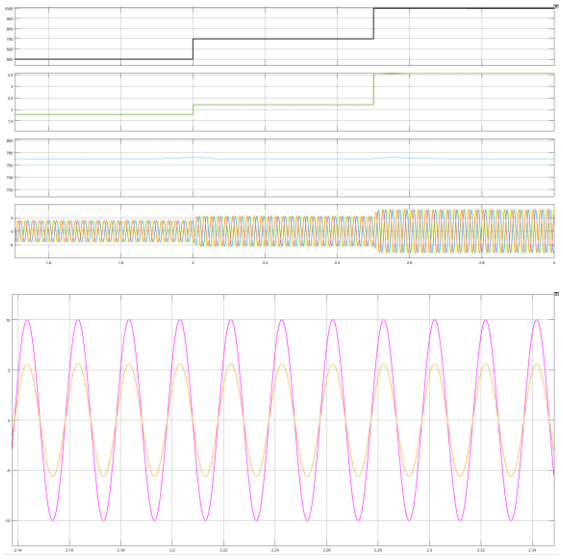

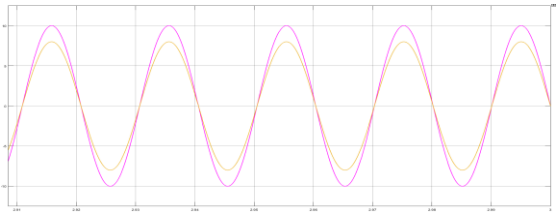

Fig.19 Simulation results of (a) step change in irradiance (b) PV current (IPV1) (c) Total DC-link voltage (Vectoral) (d)Grid currents (Gab). (e) Grid voltage (Vega) and grid current (Igga) at 700w/m^2 and 100 W/m^2.

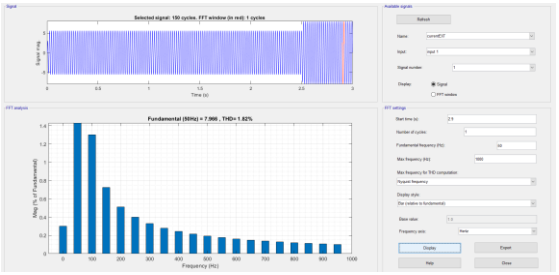

Fig.19 THD% Grid current

COMPARISION TABLE

	Existing system	Extension system
Grid current THD%	4.28%	1.82%

CONCLUSION

This paper proposes the Quasi-Z-Source Cascaded Four-Level Inverter for Photovoltaic Applications using a utilizing a Neural Network (NN) control technique for 3-stage yield from single-stage sunlight-based PV power transformation frameworks, both off-matrix and connected to the lattice. The front-end qasr organizations and the back-end FCMI are converged in a solitary stage power transformation. It is shown that contrasted with the power circuit geographies depicted in the previously mentioned before writing, the lift factor created by the LSPWM strategy is half higher. This power circuit arrangement is innately less convoluted and requires less parts than NPC or CHB-based frameworks. Utilizing re-enactment studies and resulting trial approval, the consistent state and dynamic ways of behaving of the proposed power converter in independent mode have been researched. Recreation and trial and error both uncover that the DC-connections of the proposed power converter might be managed by changing

ISSN- 2394-5125 VOL 7, ISSUE 01, 2020

the shoot-through obligation factor. It follows that the proposed power converter needs nothing other from the power source itself. Continuous recreations are utilized to survey the proficiency of the proposed power converter in matrix associated mode, which is constrained by a NN controller. It is exhibited that FCMI result can be controlled by means of the tweak file, and that PSO-MPPT can be carried out by means of the shoot-through obligation factor. It is shown that the proposed power converter, when joined with a PLL, can infuse the dynamic power into the lattice at UPF.

REFERENCES

[1] M. Shen, A. Joseph, J. Wang, F. Z. Peng and D. J. Adams, "Comparison of Traditional Inverters and Z -Source Inverter for Fuel Cell Vehicles," in IEEE Transactions on Power Electronics, vol. 22, no. 4, pp. 1453-1463, July 2007.

[2] N. Rana, M. Kumar, A. Ghosh and S. Banerjee, "A Novel Interleaved Tri-State Boost Converter with Lower Ripple and Improved Dynamic Response," in IEEE Transactions on Industrial Electronics, vol. 65, no. 7, pp. 5456-5465, July 2018.

[3] Y. Xue, B. Ge and F. Z. Peng, "Reliability, efficiency, and cost comparisons of MW-scale photovoltaic inverters," 2012 IEEE Energy Conversion Congress and Exposition (ECCE), Raleigh, NC, pp. 1627-1634, 2012.

[4] Fang Zheng Peng, "Z-source inverter," in IEEE Transactions on Industry Applications, vol. 39, no. 2, pp. 504-510, April 2003.

[5] Fang Zheng Peng et al., "Z-source inverter for motor drives," in IEEE Transactions on Power Electronics, vol. 20, no. 4, pp. 857- 863, July 2005.

[6] J. Anderson and F. Z. Peng, "A Class of Quasi-Z-Source Inverters," 2008 IEEE Industry Applications Society Annual Meeting, Edmonton, AB, pp. 1-7, 2008.

[7] S. Busquets-Monge, J. Robert, P. Rodriguez, S. Alexus and J. Bordonua, "Multilevel Diode-Clamped Converter for Photovoltaic Generators with Independent Voltage Control of Each Solar Array," in IEEE Transactions on Industrial Electronics, vol. 55, no. 7, pp. 2713-2723, July 2008.

[8] P. K. Kar, A. Priyadarshi, S. B. Karangi and A. Ruderman, "Voltage and Current THD Minimization of a Single-phase Multilevel Inverter with an Arbitrary RL-load Using a Time-domain Approach," in IEEE Journal of Emerging and Selected Topics in Power Electronics, Doi: 10.1109/JESTPE.2021.3050787.

[9] P. C. Loh, F. Blaabjerg and C. P. Wong, "Comparative Evaluation of Pulse width Modulation Strategies for Z-Source Neutral-Point Clamped Inverter," in IEEE Transactions on Power Electronics, vol. 22, no. 3, pp. 1005-1013, May 2007.

[10] P. C. Loh, F. Gao, F. Blaabjerg, S. Y. C. Feng and K. N. J. Soon, "Pulse Width-Modulated Z-Source Neutral-Point-Clamped Inverter," in IEEE Transactions on Industry Applications, vol. 43, no. 5, pp. 1295-1308, Sept.-Oct. 2007.

[11] P. C. Loh, S. W. Lim, F. Gao and F. Blaabjerg, "Three-Level Source Inverters Using a Single LC Impedance Network," in IEEE Transactions on Power Electronics, vol. 22, no. 2, pp. 706-711, March 2007.

[12] S. M. Dehghan, M. Mohamad Ian, A. Yadean and F. Ashraf Zadeh, "Dual-input dual-output z-source inverter," 2009 IEEE Energy Conversion Congress and Exposition, USA, pp. 3668-3674, 2009.

[13] O. Husev, C. Roncero- Clemente, E. Romero- Cadaval, Dianion, and S. Ostapenko, "Single phase three- level neutral- point- clamped quasi- Z- source inverter', IET Power Electronics, 8, (1), pp. 1–10, 2015.

[14] C. Qin, C. Zhang, A. Chen, X. Xing and G. Zhang, "A Space Vector Modulation Scheme of the Quasi-Z-Source Three-Level T-Type Inverter for Common-Mode Voltage Reduction," in IEEE Transactions on Industrial Electronics, vol. 65, no. 10, pp. 8340- 8350, Oct. 2018.

[15] S. K. Chattopadhyay and C. Chakraborty, "Three-Phase Hybrid Cascaded Multilevel Inverter Using Topological Modules With 1:7 Ratio of

ISSN- 2394-5125 VOL 7, ISSUE 01, 2020

Asymmetry," in IEEE Journal of Emerging and Selected Topics in Power Electronics, vol. 6, no. 4, pp. 2302-2314, Dec. 2018

[16] Q. Huang and A. Q. Huang, "Feed forward Proportional Carrier Based PWM for Cascaded H-Bridge PV Inverter," in IEEE Journal of Emerging and Selected Topics in Power Electronics, vol. 6, no. 4, pp. 2192-2205, Dec. 2018.

[17] T. Zhao et al., "Harmonic Compensation Strategy for Extending the Operating Range of Cascaded H-Bridge PV Inverter," in IEEE Journal of Emerging and Selected Topics in Power Electronics, vol. 8, no. 2, pp. 1341-1350, June 2020.

[18] Donges Sun, Booming Ge, F. Z. Peng, A. R. Haitham, Daqing Bi and Yushan Liu, "A new grid-connected PV system based on cascaded H-bridge quasi-Z-source inverter," 2012 IEEE International Symposium on Industrial Electronics, Hangzhou, pp. 951-956, 2012.